International Journal of Mechanical, Industrial and Aerospace Sciences
ISSN: 2517-9950
Vol:1, No:4, 2007

# Neural Network Based Icing Identification and Fault Tolerant Control of a 340 Aircraft

F. Caliskan

***Abstract*—**This paper presents a Neural Network (NN) identification of icing parameters in an A340 aircraft and a reconfiguration technique to keep the A/C performance close to the performance prior to icing. Five aircraft parameters are assumed to be considerably affected by icing. The off-line training for identifying the clear and iced dynamics is based on the Levenberg-Marquard Backpropagation algorithm. The icing parameters are located in the system matrix. The physical locations of the icing are assumed at the right and left wings. The reconfiguration is based on the technique known as the control mixer approach or pseudo inverse technique. This technique generates the new control input vector such that the A/C dynamics is not much affected by icing. In the simulations, the longitudinal and lateral dynamics of an Airbus A340 aircraft model are considered, and the stability derivatives affected by icing are identified. The simulation results show the successful NN identification of the icing parameters and the reconfigured flight dynamics having the similar performance before the icing. In other words, the destabilizing icing affect is compensated.

***Keywords*—**Aircraft Icing, Stability Derivatives, Neural Network Identification, Reconfiguration.

## I. Introduction

THE on-going research regarding ice in flight is still actual for engineers and researchers for it destroys the smooth flow of air by increasing drag while decreasing the ability of the airfoil to create lift. The actual weight of the ice on the airplane is insignificant when compared to the airflow disruption it causes. As power is added to compensate for the additional drag and the nose is lifted to maintain altitude, the angle of attack is increased, allowing the underside of the wings and fuselage to accumulate additional ice. Ice accumulates on every exposed frontal surface of the airplane—not just on the wings, propeller, and windshield, but also on the antennas, vents, intakes, and cowlings. It builds in flight where no heat or boots can reach it. It can cause antennas to vibrate so severely that they break. In moderate to severe conditions, a light aircraft can become so iced up that continued flight is impossible. The airplane may stall at much higher speeds and lower angles of attack than normal. It can roll or pitch uncontrollably, and recovery may be impossible.

F. Caliskan is with the Electrical Engineering, Istanbul Technical University 34436, Istanbul, Turkey (phone: 90-212-2853683; fax: 90-212-2856700; e-mail: caliskan@elk.itu.edu.tr).

Ice can also cause engine stoppage by either icing up the carburettor or, in the case of a fuel-injected engine, blocking the engine's air source. This paper only considers the wing icing occurrences.

NASA has performed several flight tests for in-flight icing of the aircraft DHC-6 Twin Otter since 1986. Ratvasky and Ranauda [1] obtained very useful data regarding the effects of aircraft icing to aircraft stability and control in early 1990. As soon as aircraft icing was announced as a prior issue in 1997, NASA established a team called Icing Research Group. Bragg, Perkins, Sarter, Başar, Voulgaris, Gurbacki, Melody, Selig and McCray [2], [3] from Illinois University investigated aircraft icing from several different viewpoints and proposed a Smart Icing System. Miller and Ribben [4] tried to detect tail icing by evaluating the decrease of elevator effectiveness via a failure detection filter. In another application, these researchers used a state estimator as a type of Luenberger Observer. These studies showed that icing detection via statistical error analysis of states was more effective than online parameter estimation. With NASA support, Ratvasky and Zante [5] examined experimentally and analytically the effects of tail icing. Bragg et al. [6] proposed a method for flight envelope protection by identifying icing characterization. Melody, et al. [7], [8] applied H-infinity algorithm to icing identification problem. They claimed that the proposed method is better than least square estimation and Extended Kalman Filter methods. Schuchard et al. [9] worked on tail icing detection and classification by estimating icing affected parameters and sensor information via neural networks. Johnson and Rokhsaz [10] proposed a method detecting icing via neural networks and Kohonen Self Organizing Maps (SOMs). By observing neural network connection weights' changes, they tried to find iced and clean aircraft model via SOMs. They presented the effects of atmospheric turbulences and elevator input signal to icing identification.

With respect to identification of degradation in aerodynamic parameters and characteristics of flight dynamics due to aircraft icing, Dynamic Icing Detection System (DIDS) was proposed by Myers et al. [11]. Bragg et al. [2], [6], [3] used hinge moment sensors in order to detect icing on control surfaces. They developed a neural network model to estimate stability and control derivatives.

This study handles icing identification and reconfiguration together. Reconfiguration based on control mixer approach has been interest of several researchers (Rattan [12], Hajiyev and Caliskan [13]). The new gain matrix is obtained to determine the reconfigured control law such that the dynamics

of the reconfigured system is as close to the unimpaired system dynamics as possible.

## II. A340 Aircraft Model

An in-flight icing identification and reconfiguration procedure is designed and applied to an unstable multi-input multi-output model of an Airbus 340. The aircraft is stabilized by means of a standard linear quadratic optimal controller. The flight of aircraft TC-JDM in Turkish Airlines, flying at 30000 feet height over South Asia on 30 March 2003, is chosen as the model. From take-off to landing, all flight data of 2.5-hour flight are downloaded from Flight Data Recorder (FDR) (Aykan [14]). By using these flight data, stability and control derivatives are calculated according to the procedures described as in Roskam [15] and Advanced Aircraft Analysis [16], and the state-space model of the aircraft is obtained as follows:

$$\mathbf{x}(k+1) = \mathbf{A}\mathbf{x}(k) + \mathbf{B}\mathbf{u}(k) + \mathbf{G}\mathbf{w}(k) \quad (1)$$

where **A** is the system matrix, **B** is the control distribution matrix, **u** is the control input vector, and **w** is the system noise vector with the following statistical characteristics;

$$E[\mathbf{w}(k)] = 0; \quad E[\mathbf{w}(k)\,\mathbf{w}^T(j)] = \mathbf{Q}(k)\delta(kj) \quad (2)$$

**G** is the transition matrix of system noise, and δ(kj) is the Kronecker symbol. The aircraft state variables are:

$$\mathbf{x} = [v \quad \alpha \quad q \quad \theta \quad \beta \quad p \quad r \quad \phi \quad \Psi]^T \quad (3)$$

where, v is the forward velocity, α is the angle of attack, q is the pitch rate, θ is the pitch angle, β is the side-slip angle, p is the roll rate, r is the yaw rate, ϕ is the roll angle, and ψ is the yaw angle. The aircraft model has four control surfaces and four control inputs are:

$$\mathbf{u} = [\delta_H \quad \delta_E \quad \delta_A \quad \delta_R] \quad (4)$$

where $\delta_h$ , $\delta_e$ , $\delta_a$ and $\delta_r$ are the deflections of stabilizer, elevator, aileron and rudder, respectively. The system and control distribution matrices are as in [14].

The measurement vector can be written as:

$$\mathbf{y}(k) = \mathbf{C}\,\mathbf{x}(k) + \mathbf{v}(k) \quad (5)$$

where **C** is the measurement matrix, which is a 9x9 unit matrix, **v**(k) is the measurement disturbance, and its mean and correlation matrix respectively are:

$$E[\mathbf{v}(k)] = 0; \quad E[\mathbf{v}(k)\,\mathbf{v}^T(j)] = \mathbf{R}(k)\delta(kj) \quad (6)$$

## III. Parameters Affected by Icing

Icing results in decreasing aircraft aerodynamic performance which are affected by changes in lift, drag and pitch moment, and their effectiveness with regard to aircraft position angles and velocities. This effect may be reflected in stability and control derivatives in the aircraft linearized dynamic equations. The researches in NASA Icing Research Group and Icing Institute of Illinois University (Melody et al. [17]) showed that the most affected parameters from in-flight wing icing are:

$$C_{D_\alpha} = \frac{\partial C_D}{\partial \alpha},\ C_{L_\alpha} = \frac{\partial C_L}{\partial \alpha},\ C_{L_q} = \frac{\partial C_L}{\partial q},\ C_{M_\alpha} = \frac{\partial C_M}{\partial \alpha},\ C_{M_q} = \frac{\partial C_M}{\partial q} \quad (7)$$

where $C_{D_\alpha}$, $C_{L_\alpha}$, $C_{L_q}$, $C_{M_\alpha}$, and $C_{M_q}$ are stability derivatives; $C_D$, $C_L$, $C_M$ are drag, lift and pitch moment coefficients, respectively. The derivative of lift coefficient with respect to angle of attack, $C_{L_\alpha}$, includes the components due to the wing, the fuselage, and the tail for the total airframe.

When aircraft linearized equations are examined, it is easily found that all these derivatives are in the matrix **A**. Considerably affected parameters are included in the elements **A**(1,2), **A**(2,2), **A**(2,3), **A**(3,2), **A**(3,3), and can be written as; $\mathbf{A}(1,2) = k_1(C_{D_\alpha} - C_L)$, $\mathbf{A}(2,2) = k_2(C_{L_\alpha} + C_D)$, $\mathbf{A}(2,3) = k_3 C_{L_q}$, $\mathbf{A}(3,2) = k_4 C_{M_\alpha}$, $\mathbf{A}(3,3) = k_5 C_{M_q}$ where $k_i$, i=1,2,3,4,5, consists of all other flight parameters which are considered constant for a certain time interval. These constants may be calculated from certain flight conditions such as take off, climb, cruise, and landing.

In the simulations in Section 6, **A**(1,2), **A**(2,2), **A**(2,3), **A**(3,2), and **A**(3,3) are expressed as $a_{12}$, $a_{22}$, $a_{23}$, $a_{32}$, and $a_{33}$, respectively. In this study, duration of two minutes, four ice-affected parameters are assumed to decrease their halves, and one parameter to increase fifty percent more in parallel to studies in the literature (Brag et al. [6], McLean [18]).

## IV. Design of Neural Network Model to Estimate Icing Affected Parameters

Schuchard et al. [9] introduced a neural network system that detects and classifies aircraft ice accretion in order to improve flight performance and safety. Neural networks are developed for use within an ice management system that monitors icing and its effects upon performance, stability and control.

Neural networks have increasingly been shown as viable tools for mapping nonlinear systems and for the purpose of parameter identification. It is very efficient method in the analysis of nonlinear and complex models if enough data are available for its training phase. Unfortunately, there is no enough training data available regarding stability and control derivatives. There are little data only for a few research aircraft obtained from tunnel tests or flight tests. After enough data are picked up from other methods, neural networks may be used effectively for control. This study aims to generate reconfigured control vector followed by identifying the stability derivatives of iced configuration.

A quick response in a certain time frame is especially critical for icing determination since ice accretion during flight at low altitude requires immediate action. NNs also have the capability to be trained on-line using real data or off-line with recorded or simulated data (Campa et al. [19]).

In this study, since there are nine states measured and five parameters to be estimated, a neural network structure having nine inputs from the Kalman filter and five outputs is

presented as shown in Fig. 1. Input and output layers have sigmoid and linear activation functions, respectively.

The data to train the NN are generated by simulation as follows: first icing parameters are assumed fixed and the states are observed. Then the observed states are used as inputs to the NN to estimate the weights to give the icing parameters.

For training method the Levenberg-Marquardt Backpropagation algorithm is used to maintain second-order training speed without having to compute the Hessian matrix, **H**. When the performance function has the form of a sum of squares (as is typical in training feedforward networks), then the Hessian matrix can be approximated as

$$\mathbf{H} = \mathbf{J}^T \mathbf{J} \tag{8}$$

and the gradient, **g**, can be computed as

$$\mathbf{g} = \mathbf{J}^T \mathbf{e} \tag{9}$$

where **J** is the Jacobian matrix that contains first derivatives of the network errors with respect to the weights and biases, and **e** is a vector of network errors. The Jacobian matrix can be computed through a standard backpropagation technique that is much less complex than computing the Hessian matrix.

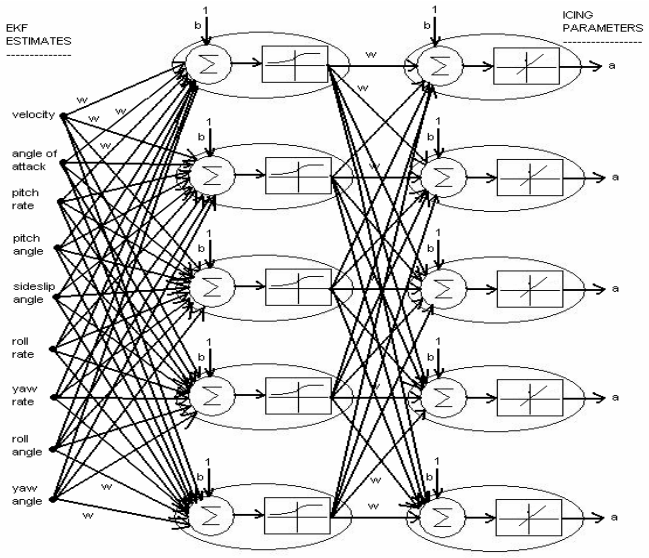


Fig. 1 Structure of neural network for icing identification

The Levenberg-Marquardt Algorithm (LMA) uses this approximation to the Hessian matrix in the following Newton-like update:

$$\mathbf{NW}_{k+1} = \mathbf{NW}_k - \left[\mathbf{J}^T \mathbf{J} + \mu \mathbf{I}\right]^{-1} \mathbf{J}^T \mathbf{e} \tag{10}$$

where $\mathbf{NW}_k$ is a vector of current weights and biases, and $\mu$ is the parameter of LMA to make the network faster and more accurate every step forward since $\mu$ can be assigned to allow that the above matrix has an inverse. If $\mu$ is zero, the method becomes the basic Newton's optimization method. When $\mu$ is large, this becomes gradient descent with a small step size. Newton's method is quicker and more accurate near an error minimum. Therefore, the aim in LMA is to shift towards Newton's method as quickly as possible.

## V. Control Mixer Approach for Reconfiguration

Reconfiguration of the control law after control surface faults has been applied by several researchers (Rattan [12], Yang and Blanke [20], and Hajiyev and Caliskan [13]). In other words, the changes in the control distribution matrix **B** are considered. The new control vector is obtained by using the control mixer approach to determine the new gain matrix such that the dynamics of the reconfigured system is as close to the unimpaired system dynamics as possible.

If the changes only occur in the matrix **A** and the changes in the matrix **B** are negligible the technique is applied as follows:

$$\dot{\mathbf{x}}_o = (\mathbf{A}_o - \mathbf{B}\mathbf{K}_o)\mathbf{x}_o \tag{11}$$

After icing that affects the matrix **A**, the dynamics turns out to be,

$$\dot{\mathbf{x}}_i = (\mathbf{A}_i - \mathbf{B}\mathbf{K}_i)\,\mathbf{x}_i \tag{12}$$

To keep the dynamics the same as before, the following condition must be held,

$$\mathbf{A}_o - \mathbf{B}\mathbf{K}_o = \mathbf{A}_i - \mathbf{B}\mathbf{K}_i \tag{13}$$

The gain matrix for the iced system is obtained as,

$$\mathbf{K}_i = \mathbf{B}^{\#}(\mathbf{A}_i - \mathbf{A}_o + \mathbf{B}\mathbf{K}_i) \tag{14}$$

where $\mathbf{A}_o$ : nominal (non-iced) system matrix, $\mathbf{A}_i$ : iced system matrix, $\mathbf{K}_i$ : gain matrix for impaired system, $\mathbf{K}_o$ : gain matrix for unimpaired system, $\mathbf{B}^{\#}$: pseudo-inverse of the matrix **B** that can be computed as,

$$\mathbf{B}^{\#} = (\mathbf{B}^T \mathbf{B})^{-1} \mathbf{B}^T \tag{15}$$

The simulations in this paper prove that this novel modified control mixer approach can also be used when the system faults have occurred.

## VI. Simulations

### *A) Simulation Results of NN Identification*

The NN identification is applied to A340 A/C model. To compensate measurement noise levels during the system identification stage, all states are filtered through a Kalman Filter. Fig. 2 shows the 5 parameters of A340 in nominal and simulated ice conditions. As noticed from the graphs, the parameters **A**(2,2) and **A**(3,3) are most affected by icing. Furthermore, they affect most the dynamics of the system. Therefore, in the simulations, these parameter effects are observed more. Fig. 3 shows the training error and the goal. The training continues until the training error becomes less than the goal. In Fig. 4 through 6 neural network outputs at training stage for the ice affected parameters are shown. Dotted lines and solid lines represent neural network outputs and targets, respectively. Initially, the errors between the NN

outputs and targets are big. However, the errors become small after training.

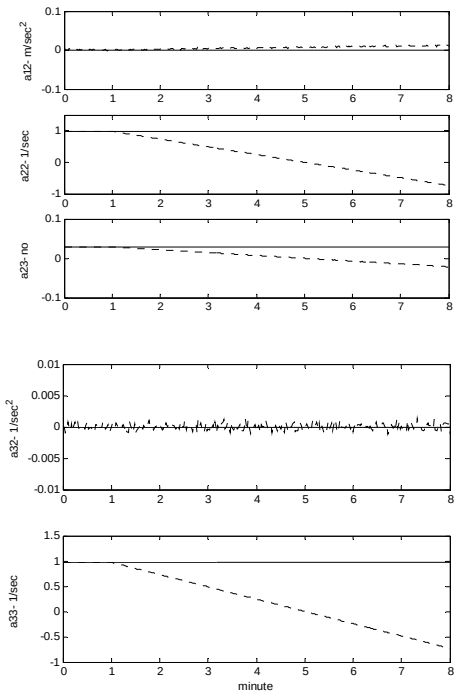


Fig. 2 Parameters of A340 in nominal and simulated ice conditions (____: nominal, - - - - : simulated)

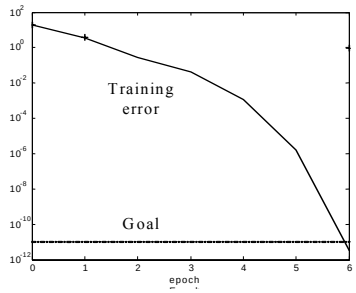


Fig. 3 Training performance

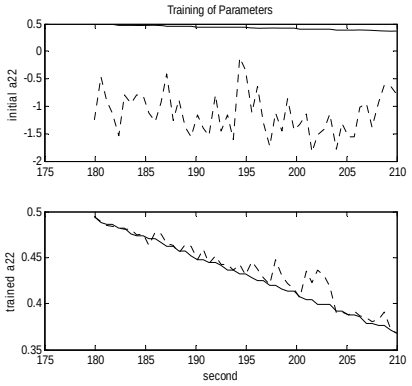


Fig. 4 Training output history of parameter $a_{22}$ (. . . . : neural network outputs, ____: targets)

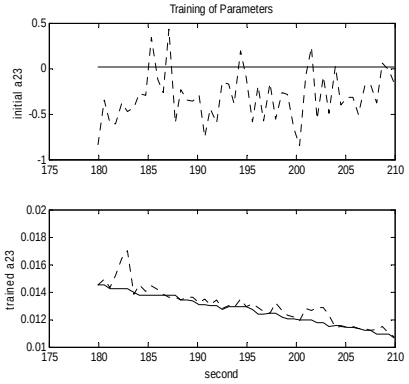


Fig. 5 Training output error history of parameter $a_{23}$ (. . . . : neural network outputs, ____: targets)

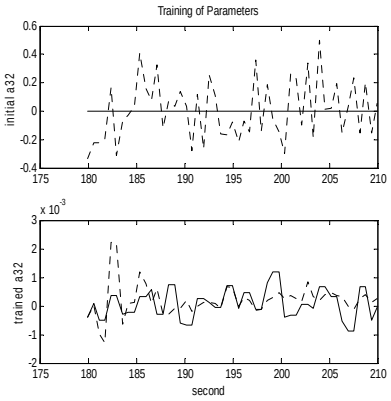


Fig. 6 Training output history of parameter $a_{32}$ (. . . . : neural network outputs, ____: targets)

### *B) Simulation Results of Control Mixer Reconfiguration*

After identifying the icing parameters of the system matrix, the control mixer approach is applied to A340 model with the iced system matrix $\mathbf{A}_i$. Although the aircraft with nominal linear quadratic control has become unstable due to icing, the reconfiguration stabilizes the system and keeps the performance very close to the one prior to icing. The control mixer approach is also compared with the new linear quadratic control and it is observed to be good enough or even better for some states. The first line in Fig. 7 shows the nominal response ( ____ ) and icing response with the nominal linear quadratic control law for $\mathbf{A}_0$ ( ._._._._ ), and the error between them. The second line in Fig. 7 shows the nominal response ( ____ ) and icing response with the new linear quadratic control law for $\mathbf{A}_i$ ( _ _ _ ), and the error between them. The third line in Fig. 7 shows the nominal response ( ____ ) and icing response with the control mixer reconfiguration for $\mathbf{A}_i$ ( . . . . ), and the error between them.

The first lines in Figs. 8-11 show the nominal response ( ____ ) and icing response with the nominal linear quadratic control law for $\mathbf{A}_0$ ( ._._._._ ). The second lines in Figs. 8-11 show the nominal response ( ____ ) and icing response with the new linear quadratic control law for $\mathbf{A}_i$ ( _ _ _ ). The third

lines in Figs. 8-11 show the nominal response ( ____ ) and icing response with the control mixer reconfiguration for $\mathbf{A}_i$ ( . . . ).

Although the states have become unstable after icing, the control mixer gain does not only stabilize them but also keeps the performance close to one prior to icing. The reconfiguration based on control mixer approach exhibits a similar performance to the linear quadratic control or even better than that.

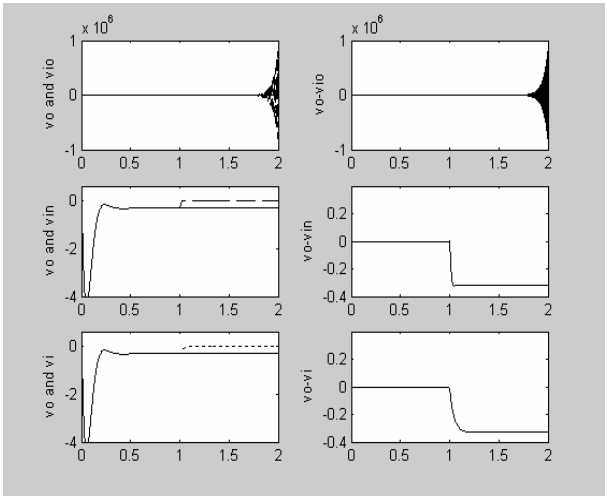


Fig. 7 Responses and errors of forward velocity for three different control laws

$v_0$: nominal forward velocity ____
$v_{i0}$: icing forward velocity with the nominal linear quadratic control ._._._
$v_{in}$: icing forward velocity with the new linear quadratic control _ _ _ _
$v_i$: icing forward velocity with the control mixer gain . . . . .

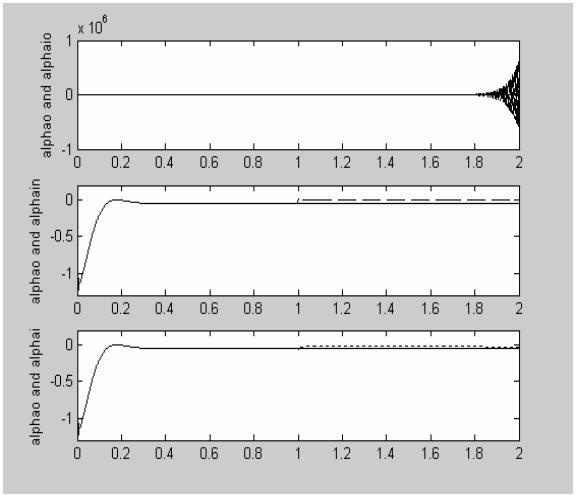


Fig. 8 Responses of angle of attack for three different control laws

$alpha_0$ : nominal angle of attack _____
$alpha_{i0}$ : icing angle of attack with the nominal linear quadratic control ._._._._
$alpha_{in}$ : icing angle of attack with the new linear quadratic control _ _ _ _ _
$alpha_i$ : icing angle of attack with the control mixer gain . . . ..

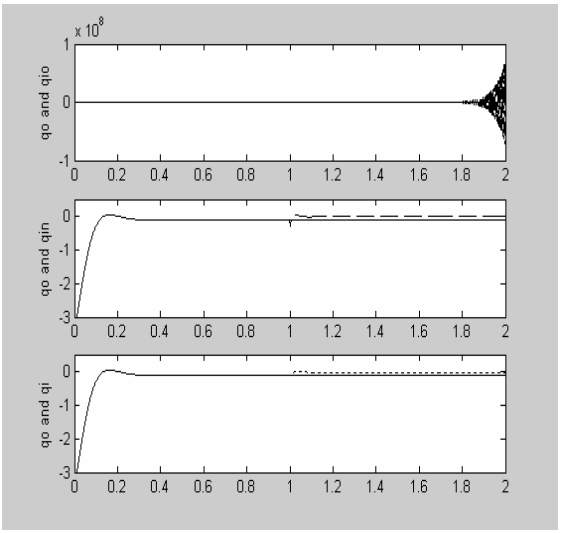


Fig. 9 Responses of pitch rate for three different control laws

$q_0$ : nominal pitch rate _____
$q_{i0}$ : icing pitch rate with the nominal linear quadratic control ._._._._._
$q_{in}$ : icing pitch rate with the new linear quadratic control _ _ _ _ _ _
$q_i$ : icing pitch rate with the control mixer gain . . . . . .

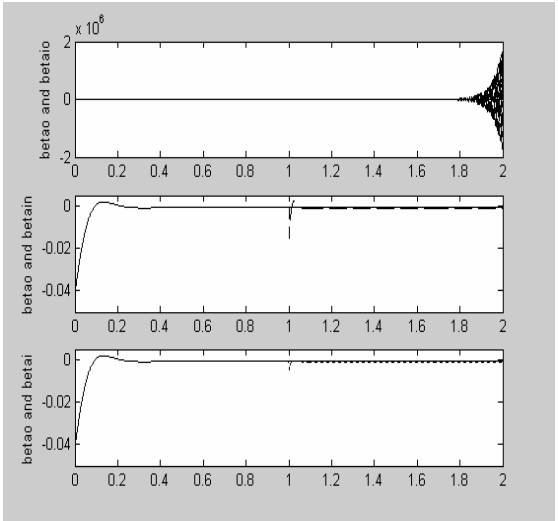


Fig. 10 Responses of side-slip angle for three different control laws

$beta_0$ : nominal side-slip angle _____
$beta_{i0}$: icing side-slip angle with the nominal linear quadratic control _._._._._
$beta_{in}$: icing side-slip angle with the new linear quadratic control _ _ _ _ _ _

$beta_i$ : icing side-slip angle with the control mixer gain . . . . . .

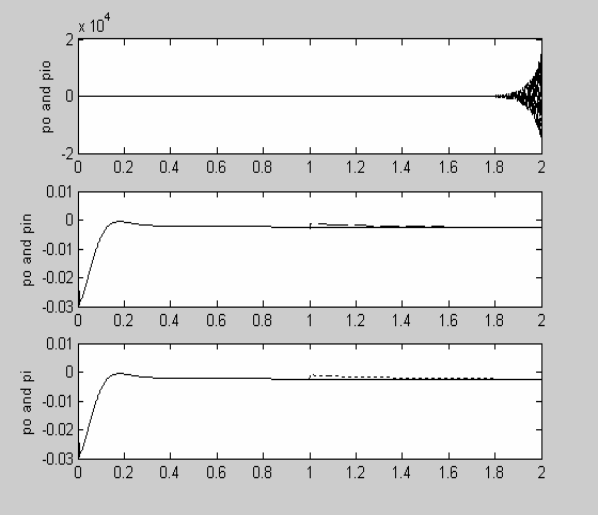


Fig. 11 Responses of roll rate for three different control laws

$p_0$ : nominal roll rate _____
$p_{i0}$ : icing roll rate with the nominal linear quadratic control _. _._._._.
$p_{in}$ : icing roll rate with the new linear quadratic control _ _ _ _ _ _
$p_i$ : icing roll rate with the control mixer gain . . . . . .

## VII. Conclusion

In this paper, the NN identification and reconfiguration of A340 aircraft subject to icing has been presented. Five parameters primarily affected by icing have been taken in accordance with the previous study results. The Levenberg Marquard Backpropogation algorithm has been used as the identification technique. The technique has been developed to estimate the aircraft stability derivatives subject to change due to icing. In the simulations, the longitudinal and lateral dynamics of an A-340 aircraft dynamic model have been considered, and the estimation of the stability derivatives affected by icing has been performed. The obtained results give an insight about that different types of icing detection are possible via the proposed method. The simulations have also shown that the modified control mixer approach could be applied to compensate for instability and performance degradation due to icing.

## References

[1] Ratvasky, T. P. and Ranaudo, R. J. (1993). Icing Effects on Aircraft Stability and Control Determined from Flight Data – Preliminary Results, NASA TM-105977 (AIAA-93-0398, 31st Aerospace Sciences Meeting and Exhibit), January.

[2] Bragg, M.B., Perkins, W.R., Sarter, N.B., Başar, T., Voulgaris, P.G., Gurbacki, H.M., Melody, J.W., and McCray, S.A. (1998). An interdisciplinary approach to in-flight aircraft icing safety, *in Proc. 36th AIAA Aerospace Sciences Meeting and Exhibit*, Reno, NV, AIAA-98-0095.

[3] Bragg, M. B., Perkins, W.R., Basar, T., Sarter, N. B., Voulgaris, P. G., Selig, M., and Melody, J. (2002). Smart Icing Systems for Aircraft Icing Safety, Reno NV, AIAA-2002-0813.

[4] Miller, R.H. and Ribbens, W.B. (1999). The Effects of Icing on the Longitudinal Dynamics of an Icing Research Aircraft. Number 99-0636 in 37th Aerospace Sciences. AIAA, January.

[5] Ratvasky, T. P. and van Zante, J. F. (1999), In-Flight Aerodynamic Measurements of an Iced Horizontal Tailplane, AIAA-99-0638, 37th Aerospace Sciences Meeting and Exhibit, January.

[6] Bragg, M.B., Hutchison, T., Oltman, R., Pokhariyal, D. and Merritt, J. (2000). Effect of ice accretion on aircraft flight dynamics, *in Proc. 38th AIAA Aerospace Sciences Meeting and Exhibit,* Reno, NV, AIAA-2000-0360.

[7] Melody, J.W., Başar, T., Perkins, W.R. and Voulgaris, P. G. (2000). H-infinity Parameter identification for inflight detection of aircraft icing, Control Engineering Practice, vol. 8, pp. 985-1001, Sept. 2000.

[8] Melody, J.W., Hillbrand, T., Başar, T., Perkins, W.R. (2001). H-Infinity Parameter Identification for In-flight Detection of Aircraft Icing: The Time Varying Case, *IFAC Control Engineering Practice*, 1327-1335.

[9] Schuchard, E. A., Melody, J. W., Başar, T., Perkins, W. R., and Voulgaris, P. (2000). Detection and classification of aircraft icing using neural networks, in Proc. 38th AIAA Aerospace Sciences Meeting and Exhibit, no. AIAA-2000-0361, (Reno, NV), Jan. 2000.

[10] Johnson, M.D., Rokhsaz, K. (2000). Using Artificial Neural Networks and Self Organizing Maps for Detection of Airframe Icing, *The 2000 Atmospheric Flight Mechanics Conference*, AIAA-2000-4099.

[11] Myers, T.T., Klyde, D.H., Magdaleno, R.E. (2000). The Dynamic Icing Detection System, *38th AIAA Aerospace Sciences Meeting and Exhibit*, Reno, NV.

[12] Rattan K.S. (1985). Reconfiguration of flight control systems after effector failure. Proceedings of Fourth International Conference on System Engineering, Coventry Polytechnic UK.

[13] Hajiyev C.M. and Caliskan F. (2001). Integrated sensor/actuator FDI and reconfigurable control for fault-tolerant flight control system design. *The Aeronautical Journal*, the Royal Aeronautical Society, England, September, pp. 525-533.

[14] Aykan, R., (2005). Aircraft icing detection, identification and reconfigurable control based on Kalman filtering and neural networks PhD. Thesis, Institute of Science and Technology, Istanbul Technical University.

[15] Roskam, J., (1982). Airplane Flight Dynamics and Automatic Flight Controls. Part I and II, Roskam Aviation and Engineering Corporation, Kansas, USA.

[16] Advanced Aircraft Analysis, Version 2.0, Software, (1997). Design, Analysis and Research (DAR) Corporation, Kansas, USA.

[17] Melody, J.W., Pokhariyal, D., Merret, J., Başar, T., Bragg, M.B. (2001). Sensor Integration for In-flight Icing Characterization Using Neural Networks, *39th Aerospace Science Meeting and Exhibit*, Reno, Nevada, AIAA-2001-0542.

[18] McLean, D. (1990). Automatic Flight Control Systems, Prentice Hall International Ltd. London, UK.

[19] Campa, G., Fravolini, M.L., Napolitano, M.R. (2002) A Library of Adaptive Neural Networks for Control Purposes, *IEEE International Symposium on Computer Aided Control System Design*, Glasgow, Scotland, UK.

[20] Yang, Z. and Blanke, M. (2000). Robust Control Mixer Module Method for Control Reconguration. Proc. of American Control Conference, Chicago, Illinois, pp. 3407-3411.